Paper No. 15-2833

Effects of Guardrail Post Deterioration on Crash Performance of Wood Post W-Beam Guardrails

Chuck Plaxico
RoadSafe, LLC
Box 312
12 Main Street
Canton, Maine 04221
Phone: (614) 578-1942, e-mail: chuck@roadsafellc.com
Malcolm H. Ray
RoadSafe, LLC
Box 312
12 Main Street
Canton, Maine 04221
Phone: (207) 514-5474, e-mail: mac@roadsafellc.com

Word count
Text = 3,825
Figures & Tables: 15 @ 250 words each = 3,750
Total number of words= 7,575

Submitted
August 1, 2015

Paper prepared for consideration for presentation and publication at the
94th Annual Meeting of the Transportation Research Board, January 2015

Paper No. 15-2833

Effects of Guardrail Post Deterioration on Crash Performance of Wood Post W-Beam Guardrails

Chuck A. Plaxico and Malcolm H. Ray

ABSTRACT

This paper presents the results of a study for developing inspection guidelines for highway maintenance engineers and maintenance supervisors to assess the level of damage and effectiveness of aged/deteriorated wood guardrail post installations based on quantitative assessment criteria. Guardrail posts with deterioration levels ranging from severe to essentially undamaged were obtained from damaged guardrail installations in Ohio. The dynamic strength properties were measured through pendulum testing. Finite element models of wood posts with various deterioration levels were developed and the constitutive behavior was calibrated based on the results of the test data from the pendulum impact study. These constitutive material models were incorporated into a validated finite element model of the G4(2W) guardrail model, and the system was evaluated under NCHRP Report 350 Test 3-11 impact conditions to quantify the effects of post degradation on the performance of the guardrail. Two damage scenarios were investigated. The first is representative of an aged guardrail system in which all the posts are deteriorated but the guardrail is otherwise undamaged. The second scenario is representative of a local repair on an aged guardrail system where a small number of the posts in an aged guardrail system are replaced with new posts. The results of this study are a set of quantitative criteria for determining the repair threshold for deteriorated wood posts for the G4(2W) strong-post guardrail system.

KEYWORDS: Guardrail Posts, Wood Deterioration, W-beam Guardrail, Numerical Simulations, Pendulum Testing, Model Validation, LS-DYNA.

INTRODUCTION

This paper presents the results of a study for developing inspection guidelines for highway maintenance engineers and maintenance supervisors to assess the level of damage and effectiveness of aged/deteriorated guardrail post installations based on quantitative assessment criteria. The guidance developed in this study builds upon the guidelines presented in NCHRP Report 656.[*Gabler10*] The primary purpose of this study was to quantify the effects of various levels of post deterioration on system performance.

The guardrail post is a fundamental component of a guardrail system and its response during a crash event is important to the overall performance of the system. The posts are intended absorb energy as they rotate through the soil during collisions. If the posts do not have sufficient strength they will fracture prematurely, resulting in excessive deflection of the w-beam rail element which may lead to rail forces that exceed its capacity. As posts deteriorate, the strength of the posts decline; thus, it is important to develop a field-assessment procedure for correlating strength degradation of guardrail posts to its effects on the crash performance of the guardrail system.

There is no particular standard at this time for quantifying the degree of rot or deterioration in a guardrail post. The approach typically used by the states is simply to replace any posts with visible deterioration under the assumption that if rot is visible there is probably also a great deal of non-visible rot; especially just below the groundline. Several non-destructive techniques have been developed which have demonstrated reasonable accuracy in predicting breaking strength of utility poles based on the modulus of elasticity of the pole. These methods include static bending tests, stress wave propagation techniques, near infrared spectroscopy, and ultrasound to name a few.[*Hron11; Tallavo09; Green06; Hendrick03; Hascall07*] In a related study, the authors developed a unique quantitative procedure for measuring the amount of deterioration of guardrail posts *in-situ* through the use of data obtained from resistograph tests on the posts. The details of that work are presented elsewhere.[*Ray15; Plaxico15*]

The objective of the current work was to quantify the effects of various levels of post deterioration on the crash performance of the guardrail system. The basic research approach entailed: (1) obtaining field-extracted wood guardrail posts from State DOT maintenance garages, (2) performing pendulum impact tests to measure the strength and capacity of the posts with various levels of deterioration, (3) developing and validating FE models of the wood posts, and (4) performing FEA simulations to quantify the effects of various levels of post deterioration (post strength degradation) on overall guardrail crash performance under impact conditions corresponding to NCHRP Report 350 test level 3.

RESEARCH APPROACH

Finite element models of wood guardrail posts with various levels of deterioration damage were developed. These models were then used in full-scale crash simulations of the G4(2W) guardrail under Report 350 Test 3-11 impact conditions to quantify the effects of post degradation on the performance of the guardrail system. The G4(2W) model used for this study was developed based on the NCHRP Report 350 TL3 compliance test for the guardrail conducted at TTI (i.e., Test 471470-26).[*Mak99*] The guardrail model consisted of twelve 13.5 feet lengths of 12-gauge w-beam rail, twenty-four 6x8x64 inch wood posts, and twenty-four 6x8x13 inch wood blockouts. The posts were spaced at 75 inches center-to-center and the w-beam rail was positioned such that the top of rail was 27-5/8 inches above ground. The posts were embedded 36 inches in the ground. The total length of the guardrail model (not including end anchors) was 151 ft.

The development and validation of the finite element model of the G4(2W) guardrail has been presented elsewhere and is not repeated here due to paper length constraints.[*Ray15*]. The various components of the validated G4(2W) guardrail model were modeled according to their baseline conditions, including the wood post model. For example, the material properties for the baseline guardrail post model were determined through the process of trial and error by comparing the dynamic impact response of the post model to the results of full-scale pendulum impact tests on new guardrail posts. This same approach was adopted here for calibrating the material properties of the wood for various levels of deterioration damage.

The data used for calibrating the properties of the deteriorated posts were derived from pendulum impact tests on aged/deteriorated guardrail posts. The posts were extracted from damaged guardrail installations in Ohio and had round cross-sections with diameters ranging from 6.45 inches to 9.15 inches with standard deviation of 0.62 inches. The tests involved a 2,372-lb rigid pendulum impacting the posts at a nominal impact speed of 10 mph at a height of 21.5 inches above ground.

The tests were performed with the posts installed in a rigid steel sleeve, as shown in Figure 1. The sleeve was a 12 x 12 x ¼ inch steel tube fabricated from A500 Class B 58,000 psi structural steel. The top of the tube was reinforced with a 5-inch tall 13 x 13 x ½ inch steel tube welded to the main tube sleeve. The foundation sleeve was braced against the steel reinforced concrete wall on the inside of the ground-pit using a 7.4 feet long S20x86 structural steel section. The posts were mounted inside the sleeve at a nominal depth of 38 inches. The posts were held in place inside the sleeve using structural grade 2x8 inch pine boards that were press-fit against the back-side of the sleeve using a 1.0-inch diameter grade 8 set-screw. Additional details regarding the pendulum test program can be found in Plaxico *et. al.*[Plaxico15]

Figure 1. Rigid steel sleeve used for post mounting.

The calibrated wood post models were then incorporated into the finite element model of the validated G4(2W) guardrail model to evaluate the effects of guardrail post deterioration on the crash performance of the system.

WOOD POST DETERIORATION DAMAGE LEVELS

Four levels of deterioration for wood guardrail posts were established based on the results of the pendulum impact tests and are presented in Table 1 in terms of force and energy capacities.[*Ray15; Plaxico15*] Figure 2 shows the results from three representative tests for the three deterioration levels DL1, DL2 and DL3. The last column of Table 1 presents the damage levels of the post in terms of relative capacity. Therefore, if post strength is measured or otherwise determined in the field via alternative means (e.g., stress wave techniques, force-deflection techniques, etc.) then the relative capacity may be used to identify damage level.

Table 1. Damage levels for guardrail post deterioration.

Damage Level	Capacity		
	Peak Force (kips)	Strain Energy (kip-in)	Relative Capacity
0 (new)	> 14	> 35	100%
1	12 - 15	26 - 40	75%
2	7 - 13	20 - 30	55%
3	< 9	< 20	< 45%

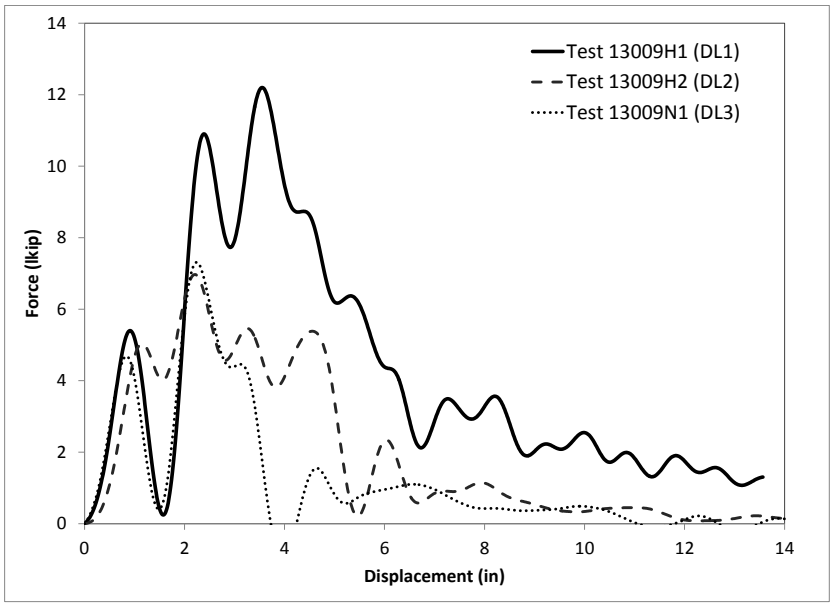

Figure 2. Pendulum test results corresponding to deterioration damage level.

CALIBRATION OF FE MODELS FOR DETERIORATED POSTS

Damage Level 1 (DL1)

The impact conditions for tests series 13009 were simulated using the finite element model shown in Figure 3. The guardrail post was modeled with a diameter of 8 inches. The material properties for damage level 1 were developed based on comparison to Test 13009H1 which resulted in a relatively low peak force with ductile post-peak failure response. The specific property values for this model are shown in Table 2 which correspond to material model *MAT_WOOD in LS-DYNA.

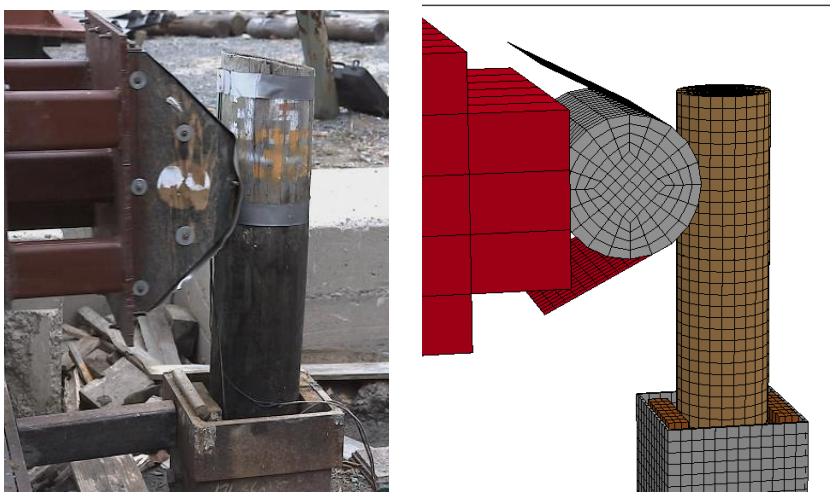

Figure 3. Finite element model used for calibrating material property values for various deterioration levels of wood posts.

Table 2. Material properties for wood post model corresponding to damage levels 1 through 3.

Variable	Description	DL1	DL2	DL3
General				
RO	Density (Mg/mm^3)	6.73E-10	6.73E-10	6.73E-10
NPLOT	Parallel damage written to D3PLOT	1	1	1
ITERS	Number of plasticity iterations	1	1	1
IRATE	Rate effects (0=off; 1=on)	1	1	1
GHARD	Perfect plasticity override (0=perfect plasticity)	0.05	0.05	0.05
IFAIL	Erosion perpendicular to grain (0=No; 1=Yes)	1	1	1
IVOL	Erode on negative volume (0=No; 1=Yes)	0	0	0
Stiffness				
EL	Parallel Normal Modulus (MPa)	11352	5676	4541
ET	Perpendicular Normal Modulus (MPa)	246.8	123.4	98.7
GLT	Parallel Shear Modulus (MPa)	715.2	357.6	286.1
GTR	Perpendicular Shear Modulus (MPa)	87.5	43.8	35
PR	Parallel Major Poisson's Ration	0.157	0.157	0.157
Strength				
XT	Parallel Tensile Strength (MPa)	35.8	30.7	27.3
XC	Parallel Compressive Strength (MPa)	12.7	8.88	7.83
YT	Perpendicular Tensile Strength (MPa)	0.86	0.74	0.66
YC	Perpendicular Compressive Strength (MPa)	2.5	1.7	1.5
SXY	Parallel Shear Strength (MPa)	3.8	3.3	2.9
SYZ	Perpendicular Shear Strength (MPa)	5.3	4.6	4.1
Damage				
$GF1_{\parallel}$	Parallel Fracture Energy in Tension (MPa-mm)	35.8	15.4	13.7
$GF2_{\parallel}$	Parallel Fracture Energy in Shear (MPa-mm)	74.1	31.8	28.2
BFIT	Parallel Softening Parameter	30	30	30
$DMAX_{\parallel}$	Parallel Maximum Damage	0.9999	0.9999	0.9999
$GF1_{\perp}$	Perpendicular Fracture Energy in Tension (MPa-mm)	0.8	0.4	0.4
$GF2_{\perp}$	Perpendicular Fracture Energy in Compression (MPa-mm)	1.6	0.83	0.83
DFIT	Perpendicular Softening Parameter	30	30	30
$DMAX_{\perp}$	Perpendicular Maximum Damage	0.99	0.99	0.99
Rate Effects				
FLPAR	Parallel Fluidity Parameter Tension/Shear	3.96E-06	3.39E-06	3.02E-06
FLPARC	Parallel Fluidity Parameter Compression	5.65E-06	3.96E-06	3.49E-06
POWPAR	Parallel Power	0.107	0.107	0.107
FLPER	Perpendicular Fluidity Parameter Tension/Shear	8.29E-05	7.10E-05	6.31E-05
FLPERC	Perpendicular Fluidity Parameter Compression	1.18E-04	8.29E-05	7.30E-05
POWPER	Perpendicular Power	0.104	0.104	0.104
Hardening				
NPAR	Parallel Hardening Initiation	0.50	0.50	0.50
CPAR	Parallel Hareding Rate (/s)	111.1	226.8	292.2
NPER	Perpendicular Hardening Initiation	0.40	0.40	0.40
CPER	Perpendicular Hardening Rate (/s)	277.8	566.9	730.5

Units: Mg, mm, sec, N, MPa

Figure 4 shows the force vs. deflection and energy vs. deflection results for the FE model compared to Test 13009H1. The peak impact force from the analysis was 13 kips compared to 12.2 kips in the test. The total energy absorbed in the analysis at 13 inches displacement was 57 kip-inches compared to 56 kip-inches in the test.

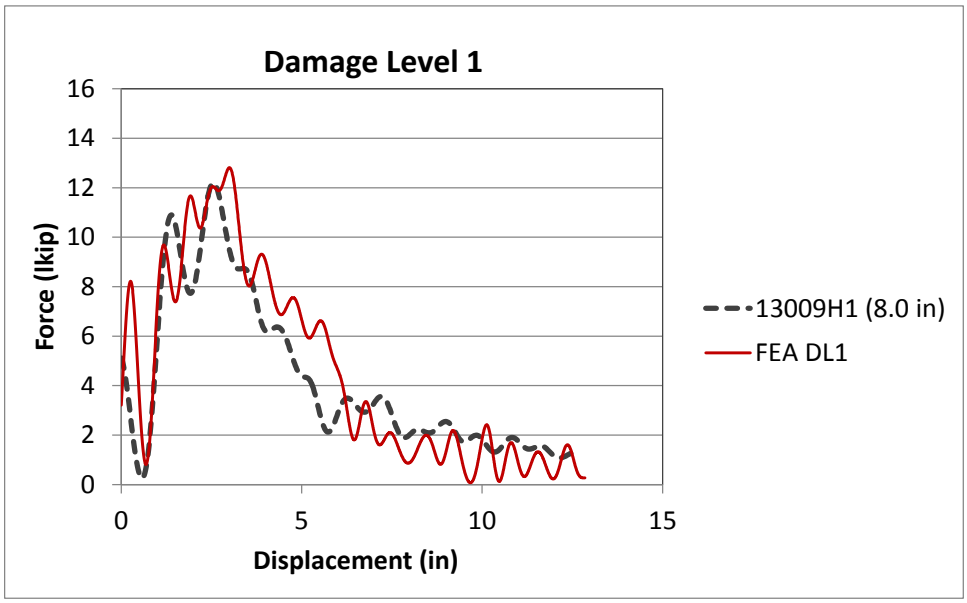

(a)

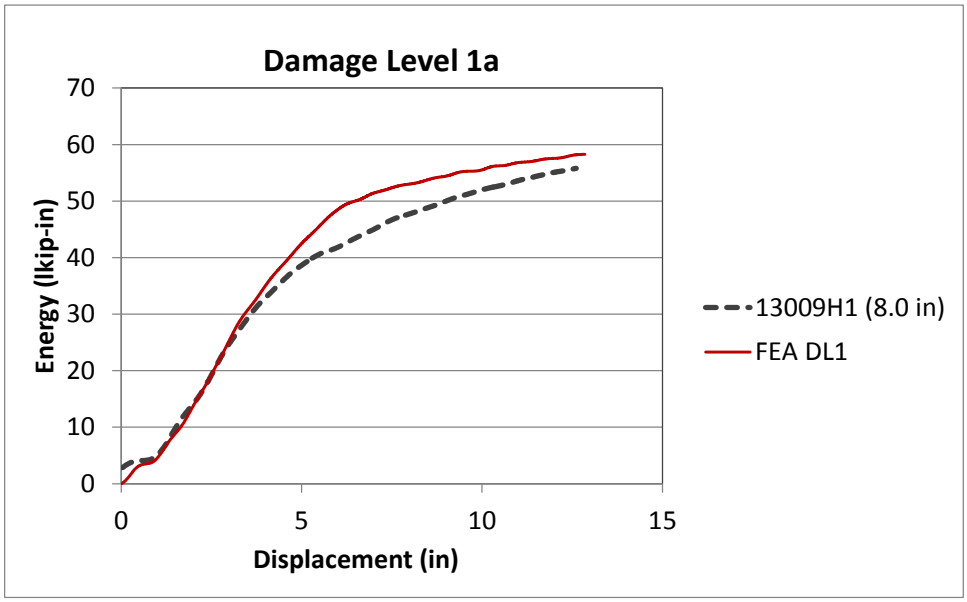

(b)

Figure 4. (a) Force vs. deflection and (b) energy vs. deflection for wood post model corresponding to Damage Level 1.

Damage Level 2 (DL2)

A single set of material properties were developed for simulating damage level 2. These properties, shown in Table 2 under heading DL2, correspond to predefined values for *MAT_WOOD_PINE with Q_T=0.36 and Q_C=0.42, with the elastic properties scaled by 50 percent of the default undamaged wood values. The impact response for this model was very similar to the results from Tests 13009Z1 and 13009H2. Figure 5 show the force vs. deflection and energy vs. deflection results for the FE model compared to the pendulum tests. The peak impact force from the analysis was 8.8 kips and the total energy absorbed in the analysis at 15 inches displacement was 27.3 kip-inches. Thus, response falls within the criteria defined for damage level 2.

Damage Level 3 (DL3)

The properties shown in Table 2 under heading DL3, correspond to predefined values for *MAT_WOOD_PINE with Q_T=0.32 and Q_C=0.37, with the elastic properties scaled by 40 percent of the default undamaged wood values. The impact response for this model was very similar to the results from Tests 13009S1. Figure 6 shows the force and energy vs. deflection results for the FE model compared to the pendulum tests. The peak impact force from the analysis was 8.4 kips, and the total energy absorbed at 15 inches displacement was 19.4 kip-inches. Thus, the response of the model falls within the criteria defined for damage level 3.

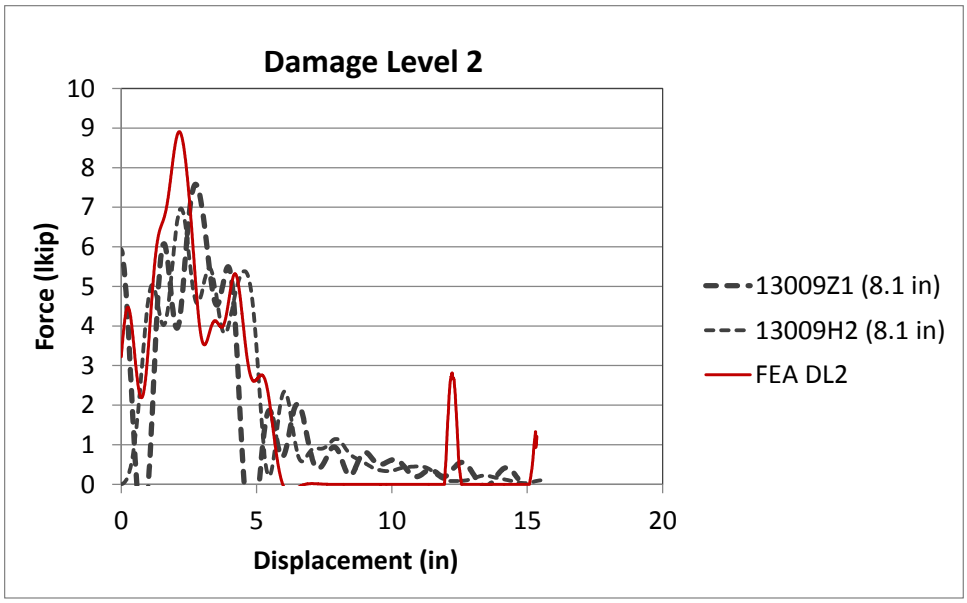

(a)

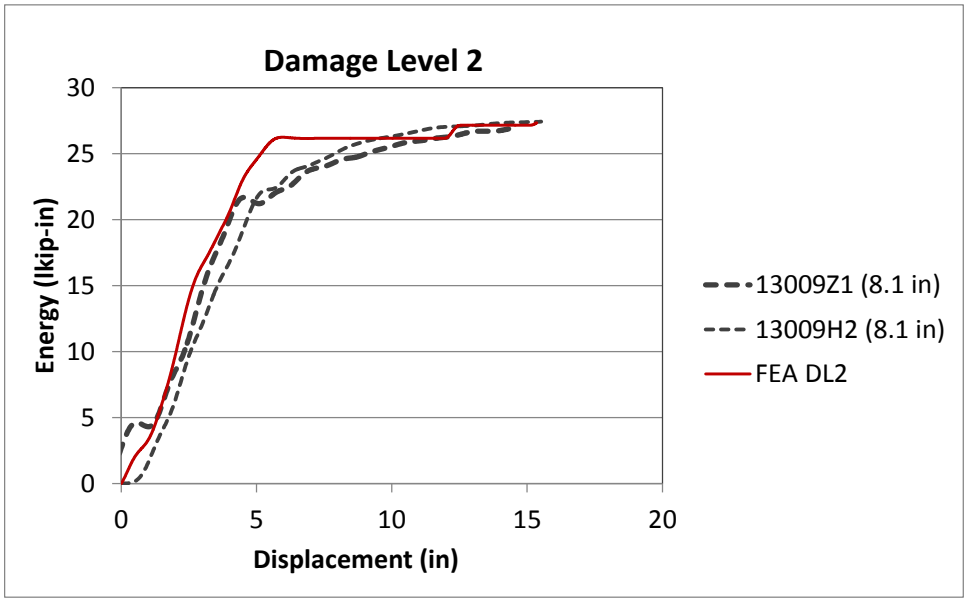

(b)

Figure 5. (a) Force vs. deflection and (b) energy vs. deflection for wood post model corresponding to Damage Level 2.

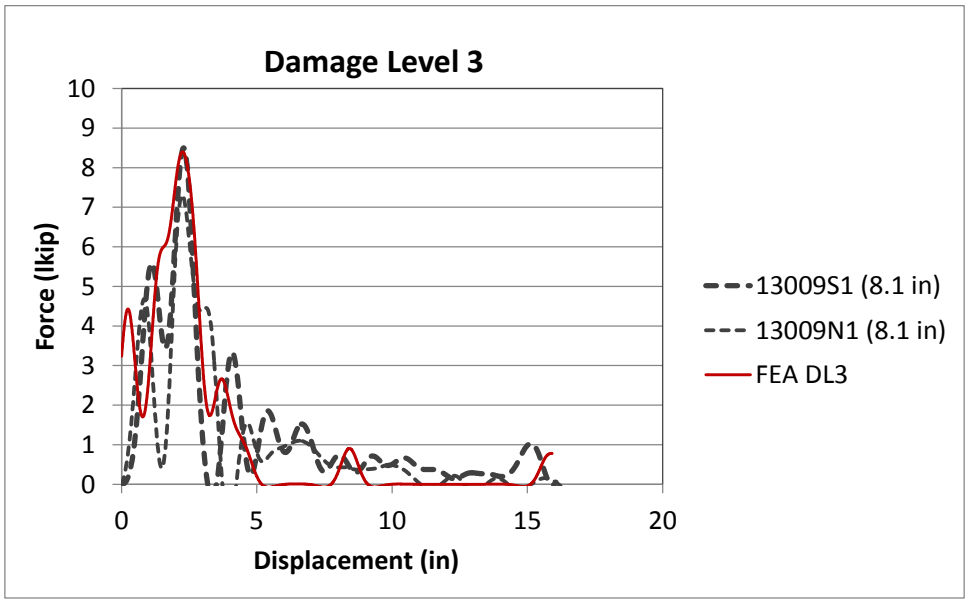

(a)

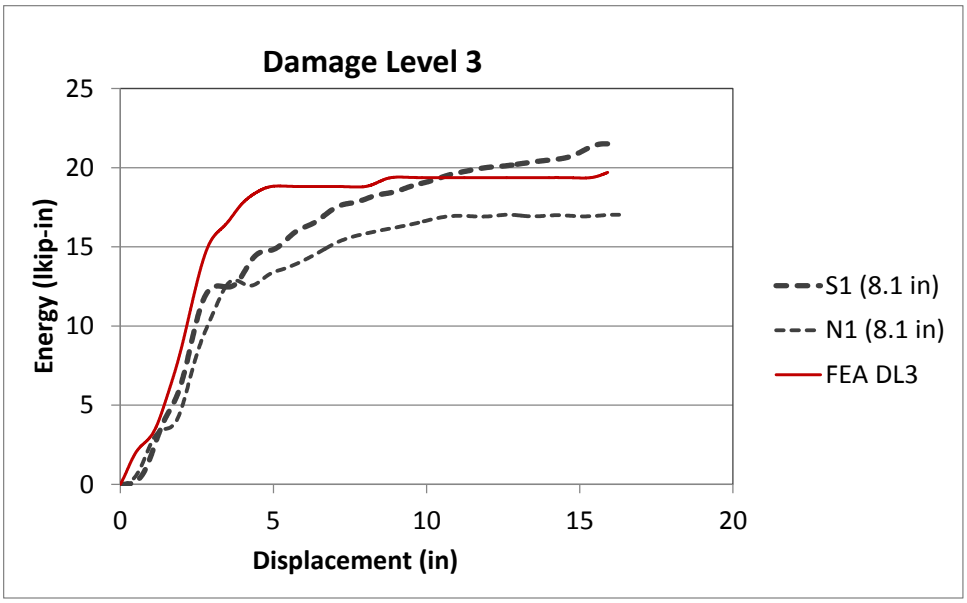

(b)

Figure 6. (a) Force vs. deflection and (b) energy vs. deflection for wood post model corresponding to Damage Level 3.

EVALUATE EFFECTS OF POST DETERIORATION ON GUARDRAIL PERFORMANCE

The effects of post strength degradation on the crash performance of the G4(2W) guardrail was evaluated using FEA. Two damage scenarios were investigated. The first involved evaluation of the G4(2W) with *uniform deterioration of the guardrail posts throughout the impact region*. This scenario is analogous to an aged guardrail system with deteriorated posts, but otherwise the guardrail is undamaged. The second scenario involved evaluation of the G4(2W) in which *a number of new posts were installed downstream and adjacent to a line of deteriorated posts*. This scenario is representative of a local repair on an aged guardrail system, where a small number of the posts in a line of deteriorated posts have been replaced with new posts.

The impact conditions were set to those of full-scale crash test 471470-26 and involved the 4,568-lb C2500D pickup model impacting the guardrail at 62.6 mph (100.8 km/hr) at an angle of 24.3 degrees.[*Mak99*] Due to time and budget constraints, the critical impact point (CIP) for each individual guardrail damage case was not determined. The impact point for all analysis cases was set at 22 inches upstream of Post 14, which corresponded to the CIP for the baseline G4(2W) guardrail in Test 471470-26.[*Mak99*] The analyses were conducted for 0.6 seconds of the impact event.

Uniform Post Deterioration in Impact Region

The analysis model used for evaluating the effects of *uniform deterioration of the guardrail posts i*s shown in Figure 7. The posts located within the impact region were modeled using MAT143 with material properties defined according to Table 2; while the posts located outside the impact region were modeled using MAT13, which was a much simpler, less computationally demanding material model. MAT13 was not calibrated for the various levels of post deterioration. Instead, the material parameters used for MAT13 were adopted from the earlier work by Plaxico, *et.al*.[*Plaxico98*] In effect, the posts outside the impact zone should be considered undamaged, or new.

The boundary conditions for the ends of the rail were modeled using non-linear springs with force-deflection response corresponding to a standard two-foundation-tube-and-strut type anchor, which was the type of anchor used in the baseline full-scale crash test.[*Mak99*] The stiffness of the anchor for these analyses were based on the results of static pull-tests performed on guardrail end-terminals.[*Ray15*] The anchor stiffness was notably less than that of the validation model in which the stiffness properties for the boundary springs were defined based on previous work presented in [*Plaxico03*]. As a result, the baseline model (i.e., model with Damage Level 0 posts) showed slightly higher deflections than the validation model. Both cases are included in the results below for relative comparisons. Table 3 provides a summary of barrier damage from the analyses related to rail deflections, anchor movement and splice damage. The maximum rail deflection increased significantly for each damage level. The deflections for DL2 and DL3 cases were more than 75 percent higher than the baseline case.

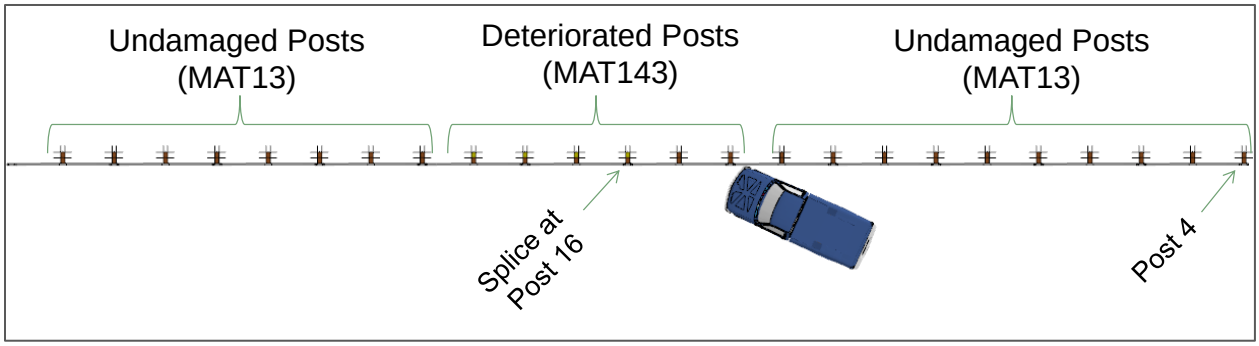

Figure 7. Analysis setup for evaluation of uniform deterioration of posts in the impact region.

Table 3. Summary of barrier damage evaluation from uniform post deterioration analyses.

Event	Validation	Analysis			
	DL0	DL0	DL1	DL2	DL3
Maximum Rail Deflection (in)	27.3	32.0	45.1	56.1	58.9
Location of Max Defl. (in) (Relative to Post 16)	-30.5	-14.8	23.8	64.4	75.0
Rail Deflection at Post 13 (in)	1.2	1.8	4.7	5.6	6.5
Rail Deflection at Post 14 (in)	11.3	13.1	20.4	22.8	24.1
Rail Deflection at Post 15 (in)	24.8	27.8	33.7	38.1	40.5
Rail Deflection at Post 16 (in)	25.4	31.1	44.3	51.4	53.9
Rail Deflection at Post 17 (in)	9.1	17.5	42.9	56.1	58.9
Rail Deflection at Post 18 (in)	0.3	1.2	32.3	54.2	56.2
Rail Deflection at Post 19 (in)	0.0	0.0	7.3	42.2	50.9
Upstream Anchor Deflection (in)	0.5	1.4	1.4	1.4	1.4
Downstream Anchor Deflection (in)	0.2	0.9	1.3	1.7	1.9
Maximum Strain in splice	0.50	0.84	1.35	1.13	1.10

For strong-post w-beam guardrails with rail splices located at the guardrail posts, the critical impact point was determined based on achieving maximum loading on a w-beam splice connection. This generally occurs when the maximum rail deflection occurs just upstream of the splice. Regarding the "location of maximum deflection" in Table 3, a negative number indicates that the maximum deflection occurred upstream of the splice at Post 16, while a positive number indicates that maximum deflection occurred downstream of the splice. The maximum rail deflection for the baseline DL0 case occurred at 14.8 inches upstream of the w-beam splice at Post 16 and can therefore be considered a critical impact case. The location of maximum deflection for the damaged post cases, on the other hand, all occurred downstream of the splice connection; particularly for cases DL2 and DL3. Thus, the results for the deteriorated post cases would likely have been more severe had a more critical impact location been used.

For the validation case, the maximum deflection was only 0.5 inches compared to 1.4 inches computed for the baseline analysis case (e.g., different anchor stiffness). For the

deteriorated post cases, the loading on the upstream anchor was essentially the same as that of the baseline analysis. The longitudinal rail deflections at the downstream anchor, however, increased significantly with each level of post deterioration. In general, higher lateral deflections in the impact region are associated with higher anchor forces. The fact that only the downstream anchor resulted in increased anchor forces is not clearly understood, but it was attributed to the fact that the location of maximum lateral deflection occurred father downstream for each increase in post deterioration level.

A summary of occupant risk measures computed from the acceleration and angular rate time-histories at the vehicle's center of gravity is provided in Table 4. The difference in results between the validation case and the baseline case is considered minimal. The results of the analyses involving deteriorated posts indicated that as post deterioration increases (i.e., post strength decreases) the vehicle decelerations decreased, thereby reducing the occupant risk metrics. This seems logical since the system is effectively becoming less stiff, similar to weak-post w-beam systems.

The potential for rail rupture was assessed by comparing the plastic strains in the w-beam rail with critical failure strain values for the w-beam material. In most rail-rupture cases, the rupture occurs at a splice connection and the tear usually passes through one or more of the splice-bolt holes.[*Bullard10; Buth99a; Buth06; Mak99b; Polivka00*] This is a strong indicator that rupture generally initiates at a splice-bolt hole. Once a tear is initiated, the tension in the rail then causes the tear to propagate vertically through the w-beam cross-section.

The failure strain for w-beam material was determined via tensile coupon tests to be approximately 0.66.[*Wright96*] Thus, when the local strains in the w-beam material at the splice-bolt holes reached a value of 0.66 it was assumed that there was a potential for tear initiation. The results indicated that the potential for splice rupture was relatively low for the validation case, with maximum plastic strain of 0.54. This was confirmed in the full-scale test in which rupture did not occur.[*Mak99*] However, for the baseline case in which the anchor stiffness was significantly reduced, the failure strain increased to 0.84. Strains of this magnitude for steel are generally associated with a high potential for material failure. In these cases, however, the strains are restricted to a very localized area at the end of the splice-bolt holes and are compressive (i.e., caused from the bearing load between the shoulder of the splice-bolt and the edge of the w-beam hole). Thus, the potential for tear initiation is much lower than the same magnitude of strain in a tensile region of the w-beam (e.g., on the upper or lower edges of the splice-bolt holes). The potential for spice rupture further increased for Case DL1 which resulted in plastic strain values reaching a magnitude of 1.35.

Table 4. Summary of occupant risk measures from evaluation of uniform post deterioration analyses.

Occupant Risk Factors		Test 471470-26	DL0 (Validation)	DL0 (Baseline)	DL1	DL2	DL3
Occupant Impact Velocity (m/s)	x-direction	4.6	5.3	5.2	4.4	3.8	3.3
	y-direction	5.8	5.8	5.3	4.8	4.3	4.3
	at time	*(0.1437 sec)*	*(0.1442 sec)*	*(0.1519 sec)*	*(0.1618 sec)*	*(0.1727 sec)*	*(0.1782 sec)*
THIV (m/s)		6.9 *(0.1404 sec)*	7.4 *0.1398*	7 0.1471	6.1 *(0.1559 sec)*	5.6 *(0.1667 sec)*	5.4 *(0.1723 sec)*
Ridedown Acceleration (g's)	x-direction	11.5 *(02025 - 0.2125 sec)*	10.2 *(0.1791 - 0.1891 sec)*	10.3 (0.1519 - 0.1619 sec)	7.9 *(0.1968 - 0.2068 sec)*	7.0 *(0.3578 - 0.3678 sec)*	5.8 *(0.27148 - 0.2814 sec)*
	y-direction	11.2 *(0.2381 - 0.2481 sec)*	11.1 *(0.2152 - 0.2252 sec)*	10.7 (0.2198 - 0.2298 sec)	8.0 *(0.2143 - 0.2243 sec)*	6.9 *(0.2825 - 0.2925 sec)*	7.3 *(0.5641 - 0.5741 sec)*
PHD (g's)		11.7 *(0.2025 - 0.2125 sec)*	13.6 *(0.2148 - 0.2248 sec)*	13.7 (0.2003 - 0.2103 sec)	8.5 *(0.2047 - 0.2147 sec)*	8.1 *(0.3571 - 0.3671 sec)*	8.7 *(0.2695 - 0.2795 sec)*
ASI		1.01 *(0.2176 - 0.2676 sec)*	0.99 *(0.1172 - 0.1672 sec)*	0.93 (0.1219 - 0.1719 sec)	0.66 (0.2062 - 0.2562 sec)	0.63 (0.2822 - 0.3322 sec)	0.65 (0.2651 - 0.3151 sec)
Max 50-ms moving avg. acc. (g's)	x-direction	6.1 *(0.1382 - 0.1882 sec)*	6.2 *(0.1390 - 0.1890 sec)*	7.6 *(0.1216 - 0.1716 sec)*	4.6 *(0.1166 - 0.1666 sec)*	3.8 *(0.3448 - 0.3948 sec)*	3.2 *(0.1808 - 0.2308 sec)*
	y-direction	6.8 *(0.0945 - 0.1445 sec)*	7.7 *(0.1179 - 0.1679 sec)*	6.5 *(0.1976 - 0.2476 sec)*	5.4 *(0.2071 - 0.2571 sec)*	5.5 *(0.2825 - 0.3325 sec)*	5.4 *(0.2661 - 0.3161 sec)*
	z-direction	9.0 *(0.2174 - 0.2674 sec)*	2.4 *(0.4155 - 0.4655 sec)*	2.4 *(0.3344 - 0.3844 sec)*	1.9 *(0.3900 - 0.4400 sec)*	1.5 *(0.3383 - 0.3883 sec)*	1.9 *(0.2985 - 0.3485 sec)*

For analysis case DL2 and DL3 the plastic strains were lower than the DL1 case but were still at magnitudes that would indicate high potential for tear initiation. It is possible, although not confirmed, that the decrease in splice damage for cases DL2 and DL3 may have been because these cases were not evaluated at the critical impact point.

Deteriorated Posts Upstream of Undamaged Posts

The analysis model used for evaluating the effects of *deteriorated posts upstream of undamaged posts* is shown in Figure 8.

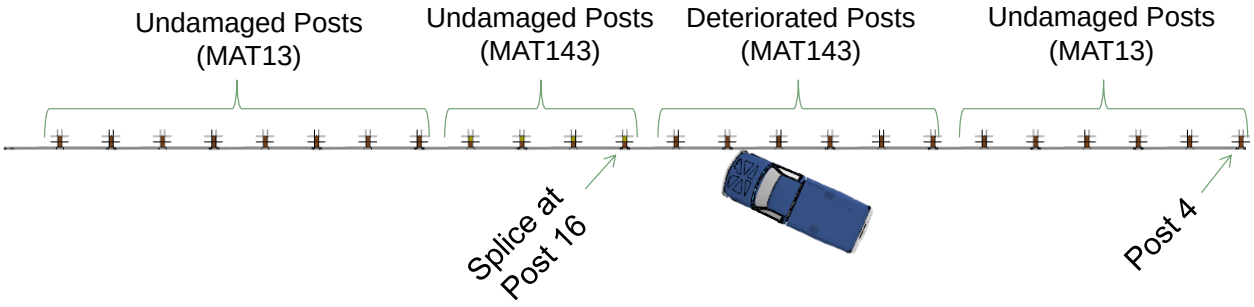

Figure 8. Analysis setup for evaluation of mixed deterioration of posts in the impact region.

Table 5 provides a summary of barrier damage from the analyses related to rail deflections, anchor movement and splice damage. The maximum rail deflection increased only slightly for the DL1 case, compared to the baseline case; while the maximum rail deflection for cases DL2 and DL3 were 46 percent and 56 percent higher than the baseline analysis case. The location of maximum rail deflection was at 21.5 inches upstream of the splice connection at Post 16 for analysis case for DL1; thus the impact conditions for this analysis were representative of the critical impact conditions. The location of maximum rail deflection for cases DL2 and DL3, on the other hand, was directly at Post 16; thus, the critical impact point for these cases was probably not achieved. It is assumed that the results for cases DL2 and DL3 would likely have been more severe had critical impact conditions been used. Based on the results from the evaluation of uniform deterioration of guardrail posts, the CIP for Case DL2 was estimated to be at approximately 20.8 feet upstream of the splice connection at Post 16, and the CIP for DL3 was estimated to be at approximately 21.7 feet upstream of the splice connection at Post 16. These impact conditions should result in maximum rail deflection occurring just upstream of the splice connection located at the first undamaged post at Post 16.

Table 5. Summary of barrier damage evaluation from mixed post deterioration analyses.

Event	Validation	Analysis			
	DL0	DL0	DL1-DL0	DL2-DL0	DL3-DL0
Maximum Rail Deflection (in)	27.3	32.0	35.5	46.6	49.8
Location of Max Defl. (in) (Relative to Post 16)	-30.5	-14.8	-21.5	0.0	0.0
Rail Deflection at Post 13 (in)	1.2	1.8	3.1	23.9	31.1
Rail Deflection at Post 14 (in)	11.3	13.1	14.2	33.2	40.3
Rail Deflection at Post 15 (in)	24.8	27.8	29.6	41.1	46.0
Rail Deflection at Post 16 (in)	25.4	31.1	34.9	46.6	49.8
Rail Deflection at Post 17 (in)	9.1	17.5	25.0	39.9	44.4
Rail Deflection at Post 18 (in)	0.3	1.2	4.6	18.9	24.6
Rail Deflection at Post 19 (in)	0.0	0.0	0.0	1.4	3.1
Upstream Anchor Deflection (in)	0.5	1.4	1.4	1.8	2.0
Downstream Anchor Deflection (in)	0.2	0.9	1.0	1.0	1.1
Maximum Strain in splice	0.50	0.84	1.00	1.16	1.27

For Case DL1 the loading on both the upstream and downstream anchors were essentially the same as those of the baseline analysis case. As the deterioration levels increased, the loading on the upstream anchor increased slightly, although deflections were not that significant (e.g., maximum deflections of 1.8 to 2 inches). The loading on the downstream anchor was essentially the same in all cases.

A summary of occupant risk measures computed from the acceleration and angular rate time-histories at the vehicle's center of gravity is provided in Table 6. The results indicate that the vehicle decelerations were very similar for all cases, with a slight trend toward decreasing values as post deterioration increased. These results seem counter intuitive and should be reassessed using a more appropriate impact point for the analyses.

The results indicated that the potential for splice rupture increased as post deterioration increased. For example, the plastic strains at the splice-bolt holes reached magnitudes of 1.0, 1.2 and 1.3 for cases DL1, DL2 and DL3, respectively. It was assumed that the results for cases DL1 and DL2 actually under-predicted the maximum strain values, since the critical impact point for these two cases was not evaluated.

Table 6. Summary of occupant risk measures from mixed post deterioration analyses.

Occupant Risk Factors		Test 471470-26	DL0 (Validation)	DL0 (Baseline)	DL1 - DL0	DL2 - DL0	DL3 - DL0
Occupant Impact Velocity (m/s)	x-direction	4.6	5.3	5.2	4.3	5.1	5.1
	y-direction	5.8	5.8	5.3	5.1	5.0	4.9
	at time	0.1437	*(0.1442 sec)*	*(0.1519 sec)*	*(0.1535 sec)*	*(0.1683 sec)*	*(0.1701 sec)*
THIV (m/s)		6.9 (0.1404 sec)	7.4 *0.1398*	7 0.1471	6.4 *(0.1484 sec)*	6.7 *(0.1629 sec)*	6.7 *(0.1646 sec)*
Ridedown Acceleration (g's)	x-direction	11.5 (02025 - 0.2125 sec)	10.2 *(0.1791 - 0.1891 sec)*	10.3 (0.1519 - 0.1619 sec)	11.2 *(0.1546 - 0.1646 sec)*	11.0 *(0.1962 - 0.2062 sec)*	9.1 *(0.1988 - 0.2088 sec)*
	y-direction	11.2 (0.2381 - 0.2481 sec)	11.1 *(0.2152 - 0.2252 sec)*	10.7 (0.2198 - 0.2298 sec)	10.2 *(0.2124 - 0.2224 sec)*	10.5 *(0.2142 - 0.2242 sec)*	7.2 *(0.2836 - 0.2936 sec)*
PHD (g's)		11.7 (0.2025 - 0.2125 sec)	13.6 *(0.2148 - 0.2248 sec)*	13.7 (0.2003 - 0.2103 sec)	13.6 *(0.1547 - 0.1647 sec)*	11.2 *(0.1964 - 0.2062 sec)*	10.0 *(0.1996 - 0.2096 sec)*
ASI		1.01 (0.2176 - 0.2676 sec)	0.99 *(0.1172 - 0.1672 sec)*	0.93 (0.1219 - 0.1719 sec)	0.89 (0.1936 - 0.2436 sec)	0.74 (0.1142 - 0.1642 sec)	0.72 (0.1145 - 0.1645 sec)
Max 50-ms moving avg. acc. (g's)	x-direction	6.1 (0.1382 - 0.1882 sec)	6.2 *(0.1390 - 0.1890 sec)*	7.6 *(0.1216 - 0.1716 sec)*	6.1 *(0.1174 - 0.1674 sec)*	5.9 *(0.1583 - 0.2083 sec)*	5.8 *(0.1939 - 0.2439 sec)*
	y-direction	6.8 (0.0945 - 0.1445 sec)	7.7 *(0.1179 - 0.1679 sec)*	6.5 *(0.1976 - 0.2476 sec)*	7.1 *(0.1919 - 0.2419 sec)*	5.6 *(0.2037 - 0.2537 sec)*	5.5 *(0.2818 - 0.3318 sec)*
	z-direction	9.0 (0.2174 - 0.2674 sec)	2.4 *(0.4155 - 0.4655 sec)*	2.4 *(0.3344 - 0.3844 sec)*	2.7 *(0.3158 - 0.3658 sec)*	2.3 *(0.3944 - 0.4444 sec)*	3.0 *(0.4245 - 0.4745 sec)*

SUMMARY AND CONCLUSIONS

The purpose of this study was to quantify the effects of various levels of wood post deterioration on the crash performance of the G4(2W) strong-post guardrail system. Guardrail posts with deterioration levels ranging from severe to essentially undamaged were obtained from damaged guardrail installations in Ohio. The dynamic strength properties of the posts were measured through pendulum testing. Finite element models of wood posts with various levels of deterioration damage were then developed and the constitutive behavior was calibrated based on the results of the test data from the pendulum impact study. These constitutive material models were incorporated into the validated G4(2W) guardrail model and the system was evaluated under NCHRP Report 350 Test 3-11 impact conditions to quantify the effects of post degradation on the performance of the guardrail.

Two damage scenarios were investigated. The first involved evaluation of the G4(2W) with *uniform deterioration of the guardrail posts throughout the impact region*. This scenario would be analogous to an aged guardrail system in which the posts are deteriorated but the guardrail is otherwise undamaged. The second scenario involved evaluation of the G4(2W) in which a number of new posts were installed adjacent to a line of deteriorated posts. This scenario is representative of a local repair on an aged guardrail system where a small number of the posts in an aged guardrail system have been replaced with new posts.

Regarding the first scenario, the analyses indicated that the lateral deflection of the rail increased significantly as post deterioration increased. As lateral rail deflection increased, the tension in the rail also increased and, consequently, resulted in higher loads on the downstream end-anchor. In this scenario, there were no indications that pocketing would be an issue. That is, as post deterioration levels increased, the system behaved more and more like a weak-post guardrail, where the posts upstream of the vehicle failed at an appropriate time, thereby preventing pocketing. However, the analyses did show that the loading on the w-beam splice at Post 16 (i.e., critical splice location for the analysis) resulted in relatively high local strains at the edges of the splice-bolt holes. The magnitude of these strains, for all cases, exceeded the failure strain of the material indicating a potential for a tear initiation. As post deterioration levels increased, the strain magnitudes increased to levels that indicated a high potential for rail rupture.

In the second damage scenario, the stiffer posts located downstream of the impact point helped to limit the lateral deflections of the rail, compared to those of the first damage scenario. In this case, the loading on the downstream anchor increased only slightly as the post deterioration levels increased, while the loading on the upstream anchor was somewhat more notable. The potential for pocketing was higher for this damage scenario and increased as post deterioration levels increased.

The critical impact point (CIP) for the undamaged G4(2W) guardrail was used for all cases. That is, the CIP was not determined for the various guardrail damage cases; thus the results presented herein are to be considered *less severe* than they might otherwise have been.

RECOMMENDATIONS

Four levels of deterioration for wood guardrail posts were defined in terms of load and energy capacity of the post data, as well as in terms of relative capacity. Therefore, if post strength is measured or otherwise determined in the field (e.g., stress wave techniques, force-deflection techniques, resistograph, etc.) then the relative capacity may be used to identify damage level.[Hron11]

As a result of this study, the authors recommend that the repair threshold for wood post deterioration be those exceeding DL2 deterioration levels. If there are hazards located within 42 inches behind the guardrail, then posts with damage levels of DL2 or greater should be replaced with high priority. Otherwise, posts with damage level DL2 are considered to be of medium priority for replacement. Posts with damage level DL3 are essentially non-functional and are considered to be of high priority for replacement. For both of these cases, the posts adjacent to the damaged posts should also be checked for damage/deterioration. If adjacent posts are DL1 or better then only the posts in the damage region need be replaced; otherwise, all the posts in the system should be replaced. A summary of the recommendations regarding wood post deterioration are presented in Table 7.

Table 7. Recommendations for wood post deterioration damage.

Damage Mode	Repair Threshold	Relative Priority
Deteriorated Posts	Posts with damage level DL3 should be replaced with high priority.	High
	If a hazard is located within 42 inches behind the w-beam rail, then posts with damage level DL2 should be replaced with high priority.	High
	Otherwise, posts with damage level DL2 should be replaced with medium priority.	Medium
	In both of these cases, the posts adjacent to the damaged posts should also be checked for damage/deterioration. If adjacent posts are DL1 or better then only the posts in the damage region need be replaced; otherwise, all the posts in the system should be replaced, due to stiffness incompatibility.	

ACKNOWLEDMENTS

This paper was based on work performed as part of National Cooperative Highway Research Program (NCHRP) Project 22-28, "Criteria for Restoration of Longitudinal Barriers, Phase II." The authors would like to thank the NCHRP for its support and the NCHRP project staff and the project panel for their comments, suggestions and direction. The authors are also indebted to the Federal Highway Administration who fully sponsored the physical testing for this study which was performed at the Federal Outdoor Impact Laboratory (FOIL) at the Federal Highway Administration's Turner Fairbank Highway Research Center (TFHRC) in McLean, Virginia. The authors would also like to thank the Ohio Department of Transportation for supplying the aged/deteriorated guardrail posts for the study.

REFERENCES

Bligh95 Bligh, R.P. and D.L. Bullard, "Crash Testing and Evaluation of Round, Wood Post, WBeam Guardrail System," Research Study No. 405391, Texas Transportation Institute, The Texas A & M University System, College Station, Texas (October 1995).

Bullard10 Bullard, D.L., Jr., R.P. Bligh, W.L. Menges, and R.R. Haug, "Volume I: Evaluation of Existing roadside Safety Hardware Using Updated Criteria – Technical Report," NCHRP Web-Only Document 157, Transportation Research Board, National Academy of Science, Washington, D.C. (2010).

Buth99a Buth, E.C., R.A. Zimmer and W.L. Menges, "Testing and Evaluation of a Modified G4(1S) guardrail with W150x17 Steel Blockouts," Test Report No. 405421-2, Texas Transportation Institute, Texas A&M University, College Station, Texas (1999).

Buth06 Buth, C.E., W.L. Menges, and S.K. Schoeneman, "NCHRP Report 350 Test 3-11 of the Long-Span Guardrail with 5.7 m Clear Span and Nested W-Beams Over 11.4 m," Report/Test No.405160-1-1, Texas Transportation Institute, College Station, Texas (May 2006).

Gabler10 Gabler, H.C., Gabauer, D.J., Hampton, "Criteria for Restoration of Longitudinal Barriers," NCHRP Report 656, Transportation Research Board, Washington, D.C. (2010).

Hascall07 Hascall, J.A., R.K. Faller, J.D. Reid, D.L. Sicking, and D.E. Kretschmann, " Investigating the Use of Small-Diameter Softwood as Guardrail Posts (Dynamic Test Results)," MwRSF Research Report No. TRP-03-179-07, Midwest Roadside Safety Facility, Lincoln, Nebraska (2007).

Hron11 Hron, J. and N. Yazdani, "Nondestructive Strength Assessment of In-Place Wood Utility Poles," *Journal of Performance of Constructed Facilities*, Vol. 25, No. 2 (April 2011).

Mak99a Mak, K.K., Bligh, R.P., and Menges, W.L., "Testing of State Roadside Safety Systems Volume XI: Appendix J – Crash Testing and Evaluation of Existing Guardrail Systems," Report No. FHWA-RD-98-046, Texas Transportation Institute, Texas A&M University System, College Station, Texas (April 1999).

Mak99b Mak, K.K., Bligh, R.P., and Menges, W.L., "Crash Testing of Ford Taurus, Chevrolet Lumina, Plymouth Neon, and Dodge Caravan – In Support of Finite Element Computer Modeling (Draft Report)", Project No. 472580, Texas Transportation Institute, Texas A&M University System, College Station, Texas (May 1999).

Plaxico98 Plaxico, C.A., Patzner, G.S., Ray, M.H., "Finite Element Modeling of Guardrail Timber Posts and the Post-Soil Interaction," *Transportation Research Record*, Paper No. 980791, Transportation Research Board, Washington D.C. (1998).

Plaxico15 Plaxico, C.A. and M.H. Ray, "Effects of Guardrail Post Deterioration on the Crash Performance of the G4(2W) Guardrail," *Transportation Research Record*, Paper No. 15-xxx (in review), Transportation Research Board, Washington D.C. (2015).

Polivka00a Polivka, K.A., R.K. Faller, D.L. Sicking, J.R. Rohde, J.D. Reid, and J.C. Holloway, "Guardrail and Guardrail Terminals Installed Over Curbs", Final Report to the Midwest States' Regional Pooled Fund Program, Transportation Research Report No. TRP-03-83-99, Project No. SPR-3(017)-Year 8, Midwest Roadside Safety Facility, University of Nebraska-Lincoln (2000).

Ray 15 Ray, M.H, C.A. Plaxico, C.E. Carrigan, and T.O. Johnson, "Criteria for Restoration of Longitudinal Barriers, Phase II," Final Report, Project 22-28, National Cooperative Highway Research Program, Washington, D.C. (expected 2015).

Wright96 Wright, A. and M.H. Ray, .Characterizing Roadside hardware Materials for LSDYNA Simulations,. *Report No. FHWA-RD-96-108*, Federal Highway Administration (1996).